Journal of Simulation and Analysis of Novel Technologies in Mechanical Engineering
14 (2) (2022) 0055~0064
HTTP://JSME.IAUKHSH.AC.IR

Research article

Indirect prediction of flank wear using ANNs in turning of CK45

Hossein Sepehri*

Department of Mechanical Engineering, Khomeinishahr Branch, Islamic Azad University, Isfahan, 84175-119, Iran

*hossein.sepehri@iaukhsh.ac.ir

(Manuscript Received --- 25 May 2022; Revised --- 12 June 2022; Accepted --- 21 June. 2022)

Abstract

This work aims to develop models to investigate the effects of flank wear on cutting forces during the turning of ck45 steel using carbide tools. Therefore, various turning experiments were performed with different cutting conditions. Flank wear and cutting forces were recorded at different stages of each experiment. The data obtained from the experiments showed that the tangential component of the cutting force was not significantly correlated with the tool flank wear. Instead, there was a good correlation between the axial and radial components of the cutting forces against flank wear. Since the cutting forces depend on both the cutting conditions and the tool flank wear, different cutting forces and cutting condition ratios were used to find the cutting force models that are more sensitive to tool wear. These ratios were used to develop artificial neural network models. The statistical results showed that the tool wear obtained from the artificial neural network models was very close to the results obtained from the experiments. In addition, the accuracy of the models including the axial component of cutting force was higher than in other models.

Keywords: Tool wear, Cutting forces, Cutting condition

1- Introduction

At present, in automated machining systems, tool wear is one of the important and influential factors in production efficiency. Knowledge of the tool's wear during the machining process will lead to better product quality based on better surface properties, more accurate geometric sizes, and better tolerances [1]. On the other hand, in systems that do not have any information about the status of the tool during the machining process, tool replacement is estimated, conservative, and based on previous data on the wear and life of the tool. In this case, the sudden failure of the tool and chipping of the cutting edge, which is common in machining processes, is not considered. Thus, in some cases, the tools have a shorter useful life and, in some cases, more than their useful life, which in the first case, the time and the cost of tool replacement increases, and

in the second case the machine tool or workpiece may be damaged [2].

Awareness of the condition of the tool and the amount of wear is done in two ways, direct and indirect [2], [3]. In direct methods, the actual amount of tool wear is measured. Various methods such as direct imaging of tool worn points [4], analysis of chips to find worn tool particles in them [5], continuous measurement of tool distance from a fixed axis [6], and resizing dimensions of Parts [7] are used for direct tool wear monitoring. In indirect methods, some parameters that are affected by tool wear, are measured, and by finding the relationship between them, the amount of tool wear is determined. Motor power [8], Electric current of main drive motor or feed motor [9], Cutting temperature [2], Roughness of machined surfaces [10], Vibration of tool [11], Changes in acoustic emission during machining [12] and cutting forces [13-22] are some of the methods that can be used to indirectly measure tool wear. The use of machining forces is one of the indirect methods of measuring tool wear. Some of the following researchers agree that the signals obtained from the machining forces contain appropriate information about the status of the machining process and their use is one of the methods of knowing the status of tool wear.

Korn and Lens [13] presented a simple mathematical model for estimating tool wear in turning. In this model, the abrasive wear of the tool is modeled by the cutting forces and the diffusion wear is modeled by using the cutting temperature. S. K. Sikdar and M. Chen [14] found that the tangential force has the largest increase with flank wear while the radial force is the smallest increase in turning of low alloy steel (AISI 4340). V.S. Sharma and others [15] analyzed the changes in cutting forces, vibrations, and acoustic emissions with cutting tool wear. They observed that the tangential component of force is more sensitive to tool wear as compared to the axial component and radial component. Using cutting force signals, Jaharah A. and others [16] develop a new regression model based on the I-Kaz method for tool wear prediction. It is shown that the three components of cutting force signals provide a sensitive measure of flank wear. V. D. Patel [17], set some turning Experiments on hardened AISI D2 steel using CBN tools with different cutting conditions (cutting speed, feed rate, and nose radius). A cutting force model is extended according to flank wear based on Waldorf's theory. The results showed that there is a close relationship between total radial cutting force and flank wear.

Recently, the use of artificial neural networks to find suitable models for tool wear and shear forces has been considered . Many researchers have considered the use of artificial neural networks to find suitable models for tool wear and cutting forces. The results of their research show that the models obtained between tool wear and cutting forces through artificial neural networks can be estimated tool wear with good accuracy based on cutting forces [18-22].

In this work, the relationship between tool flank wear and cutting forces in the turning process of ck45 steel with carbide tools is investigated (this steel is one of the most common steels and has many applications in various industries). Since the cutting forces depend on both the cutting parameters and the tool flank wear, different cutting forces and cutting parameters ratios were used to find the cutting force models that are more

sensitive to tool wear. These ratios are: Fx/A, Fx/d, Fx/f, Fy/A, Fy/d, Fy/f. In these ratios, "Fx" and "Fy" are axial and radial component forces, "A" is cutting area, "f" is feed rate and "d" is the depth of cut. These ratios were used to develop artificial neural network models.

2- Details of experiments

The scheme and the close-up view of the experimental setup are shown in Figs. 1 and 2.

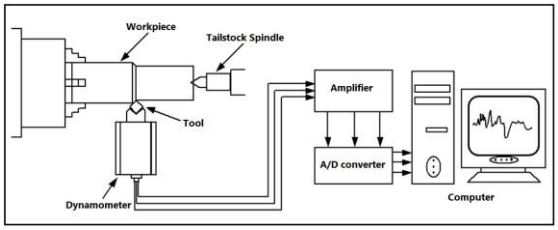

Fig. 1 Scheme of Experimental setup

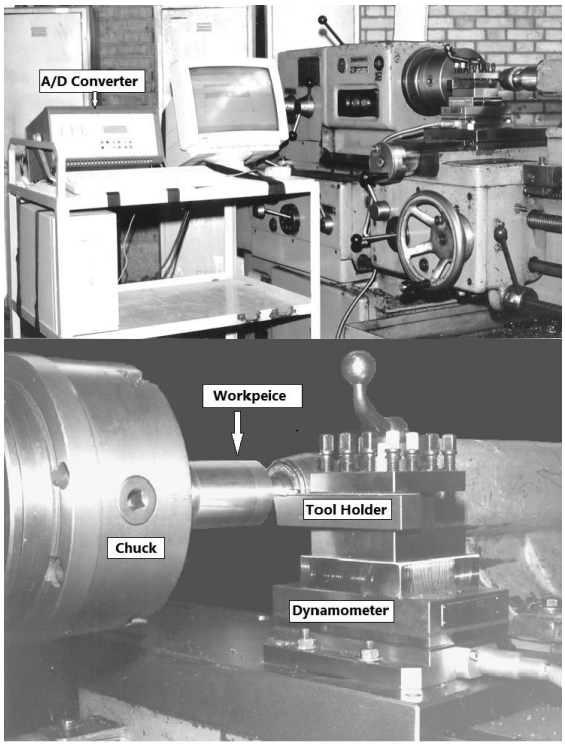

Fig. 2 Close-up view of the experimental setup

The range of cutting conditions and details of tools and materials are given in Table 1. According to the mentioned conditions, 12 experiments were designed (Table 2). Each experiment was performed in 15 stages. After each stage of the experiment, which lasted between 40 and 190 seconds, the insert was opened and the amount of flank wear was measured by an optical microscope. To measure the forces during turning, the tool holder was mounted on a piezoelectric dynamometer and the output force signals were recorded by a computer. All experiments were performed in a dry state (without lubricant or cutting fluid). To prevent the chips from twisting on the tool and increasing the forces, the chips were carefully and continuously kept away from the tool surface.

Table 1: Specification of work material, tool, and cutting conditions

Workpiece material	Ck45 82 mm×150 mm (Diameter×Long)
Cutting condition	Cutting speed: 70 ~ 190m/min Feed rate: 0.13 ~ 0.22 mm/rev Depth of cut: 1.0 ~ 1.7 mm Dry (without lubricant or cutting fluid)
Tool insert	SPUN 120308 GX(P25-P35)
Tool holder	CSDPN 25 25 M12 Back rake angle: 6° Side cutting edge angle: 5°
Dynamometer	Kistler 3-D force dynamometer (Type 9257B)

Table 2: Experimental details

No.	Depth of cut: d (mm)	Feed rate: f (mm/rev)	Cutting speed: v (m/s)	Time: t (min)
1	1	0.13	105	30
2	1	0.18	190	15
3	1	0.22	175	25
4	1.3	0.13	145	30
5	1.3	0.18	125	22
6	1.3	0.22	70	25
7	1.7	0.13	170	28
8	1.7	0.18	170	15
9	1.7	0.22	150	12
10	1.6	0.22	80	18
11	1.3	0.22	80	25
12	1.4	0.14	93	30

3- Background of artificial neural networks

Artificial neural networks are one of the common methods for detecting patterns in various manufacturing processes. They have been used to optimize processes such as casting [23], deep drawing [24], forging [25], and machining [26].

Multilayer perceptron neural networks are one of the most practical types of these networks. Fig. 3 shows a multilayer perceptron neural network that is trained whit experimental. Experiment data is entered into the neural network as input data through the first layer. Data processing is done in the middle layers. The number of middle layers can be one layer or more. The expected output data is extracted through the last layer. As shown in Fig. 3, the neural networks used in this work are of the Three Layer Perceptron type with an error backpropagation learning algorithm. In each of these networks, machining parameters include cutting speed, cutting depth, advance rate, machining time, and cutting force ratios as the first layer input and lateral wear, third layer output. The number of neurons in the middle layer to achieve optimal neural networks was determined by trial and error using EasyNN software. The training pattern of one of the neural networks is shown in Figure 5.

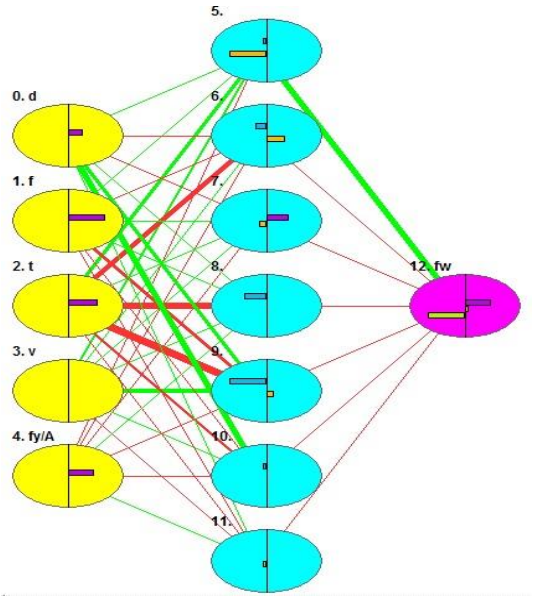

Fig. 3 Multilayer perceptron neural network
Inputs: d, f, t, v, t, Fy/A – Output: VB (flank wear)

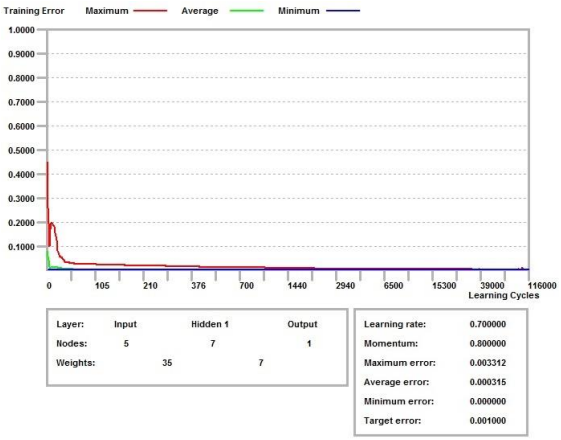

Fig. 4 Training pattern of the neural network
Inputs: d, f, t, v, t, Fx/A – Output: VB (flank wear)

4- Results and discussion

Figures 5 and 6 show a view of the tool wear area at the end of each test stage. As can be seen, the wear on the tooltip (nose wear Vc) is higher than in other areas. The average value of the wear area is considered flank wear.

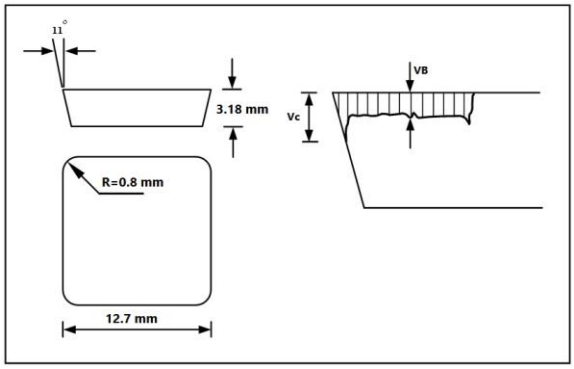

Fig. 5 Insert sizes and tool flank wear (VB)

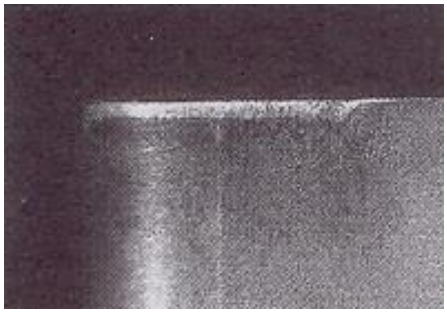

Fig. 6 Flank zone wear after the cutting condition of d=1.6 mm, f=0.22 mm, v=80m/s, t=18 min

Fig. 7-a shows the changes in the various components of the machining forces during an experiment. Large fluctuations are observed in all three components of the force. These oscillations are due to successive shocks of the grains in the workpiece to different levels of tools, light vibration tools, and other periodic oscillations during machining [28]. However, machining instabilities such as stronger seismic tools or the presence of impurities in the workpiece material cause disturbances in the force components, as shown in Fig. 7-b.

The different cutting forces in turning are shown in Fig. 8. Each of these forces can be divided into static and dynamic components [28]: F = Fs + Fd

The static component Fs is the average force fluctuations and the dynamic component Fd is the force fluctuations around the static amount of force. Changing cutting conditions (changing cutting speed, feed rate, cutting depth,

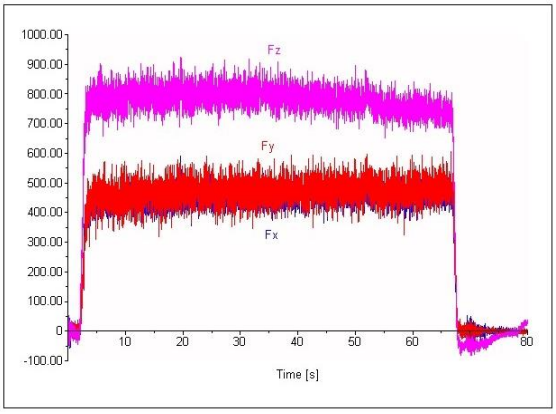

a) Normal fluctuations

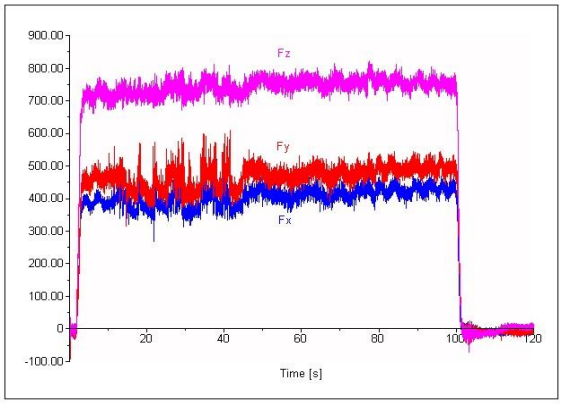

b) Abnormal fluctuations

Fig. 7 Fluctuations of cutting forces during machining

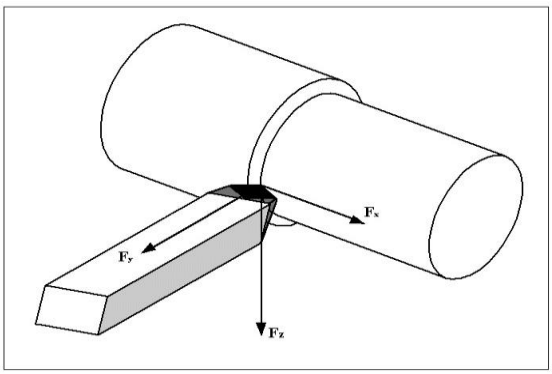

Fig. 8 Static cutting force components: F_x: Axial force (feed force), F_y: Radial force, F_z: tangential force (cutting force)

changing tool angles, etc.) as well as changing the tool wear rate, affect the dynamic and static components. The

analyzes presented in this research are based on the static components of axial force Fx, radial force Fy, and tangential (cutting) force Fz.

Figs. 9-a and 9-b show how the axial force Fx and the radial force Fy change with tool wear. As can be seen, there is an acceptable correlation between these force components and flank wear. When starting with a new tool, its edge is quickly broken, causing slight wear on the tool and increasing the initial force accordingly. The amount and rate of time of wear development in the tool depend on cutting conditions. At the end of some experiments, the width of the zone wear was about twice that of other experiments. Fig. 9-c shows how the tangential force component Fz changes with tool wear. The trend of changes in this force is initially similar to the progress of wear and incremental, but in the middle of the way, it loses its incremental trend and, in some cases, after a constant zone, decreases.

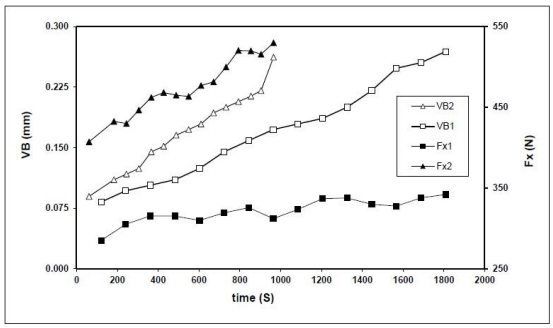

a) axial force & flank wear comparison

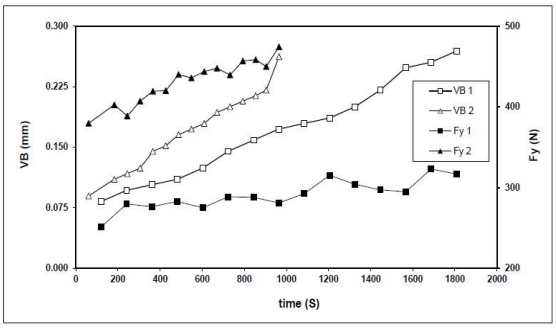

b) radial force & flank wear comparison

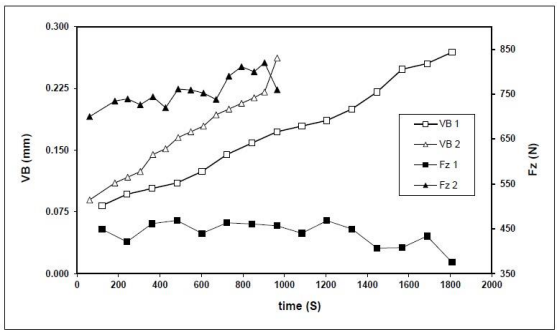

c) tangential force & flank wear comparison

Fig. 9 Cutting forces change with flank wear

cutting condition1: cutting speed=145 m/s, feed rate= 0.13 mm, depth of cut=1.3 mm

cutting condition2: cutting speed=170 m/s, feed rate= 0.18 mm, depth of cut=1.7 mm

One of the possible reasons for this can be considered as increasing the worn hole and as a result changing the cutting angle. In the first part, the size of the crater wear (area and depth) is small and occurs at some distance from the edge of the tool. In later stages, increases the area and depth of the crater wear and get closer to the tool edge. This will increase the cutting angle and naturally decrease the tangential force Fz. In this way, the effect of increasing the force due to tool wear is neutralized. In addition, the formation of a built-up edge changes the cutting conditions such as increasing the cutting angle.

According to the points mentioned, the use of Fx and Fy forces, which have a more compatible trend with changing tool wear, were used to derive the wear and force models. As mentioned earlier, since the cutting force components depend on both the cutting conditions and the tool flank wear, different cutting forces and cutting condition ratios were used to find the cutting force models that are more sensitive to tool wear. These ratios are: Fx/A, Fx/d, Fx/f, Fy/A, Fy/d, Fy/f.

According to Table 3, each of these ratios and the cutting conditions were used as input data for the first layer of artificial neural networks. Flank wear is the third layer output of artificial neural networks.

Table 3: Artificial neural network specifications

No.	Input data (first layer)	Output (third layer)	nodes in second layer	Max. error	Ave. error
1	d, f, v, t, F_x/A	VB	7	0.0039	0.0003
2	d, f, v, t, F_y/d	VB	8	0.0034	0.0003
3	d, f, v, t, F_x/f	VB	8	0.0035	0.0003
4	d, f, v, t, F_y/A	VB	7	0.0033	0.0003
5	d, f, v, t, F_x/d	VB	8	0.0032	0.0003
6	d, f, v, t, F_y/f	VB	8	0.0028	0.0003

Fig. 10 shows a comparison between the actual values obtained through two experiments and the values predicted by artificial neural networks. In these figures, the results of different patterns of artificial neural networks are compared with each other. The input of these patterns is different force ratios and cutting conditions. After training the neural networks based on the experimental data, these networks are used to estimate the amount of tool wear based on the specified cutting parameters. According to the figure, it can be seen that the models obtained from artificial neural networks correspond to the results of experiments with a good approximation.

A comparison of the Statistical analysis of artificial neural network models in table 3 is shown in table 4. As can be seen, based on the statistical coefficients RMS (Root Mean Square Error) and COV (Coefficient Of Variation), patterns 1 and 3, in which the Fx/A and Fy/A ratios are used, have better results. In the next step, there is pattern 5. Overall, according to the table above, the patterns in which Fx force ratios are used, show better results.

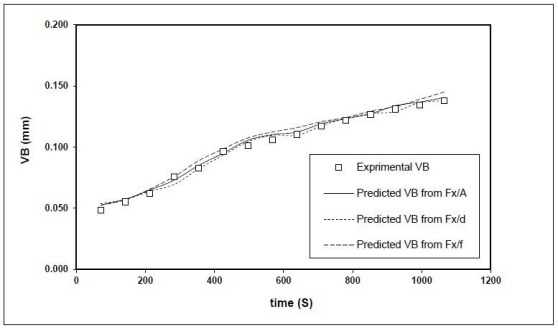

a) cutting speed=80 m/s, feed rate= 0.22 mm, depth of cut=1.6 mm

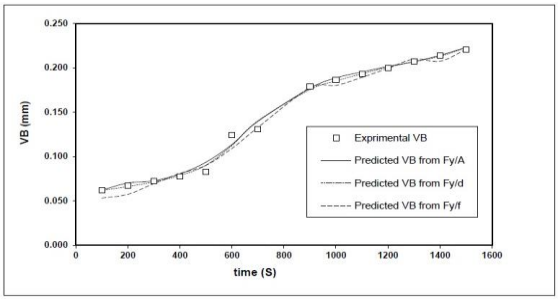

b) cutting speed=80 m/s, feed rate= 0.22 mm, depth of cut=1.3 mm

Fig. 10 comparison between experimental flank wear and predicted

Table 4: Statistical analysis of artificial neural network models of table 3

	No. of Artificial neural network					
	1	2	3	4	5	6
rms	0.0036	0.0056	0.0060	0.0035	0.0041	0.0061
cov	2.6%	4%	4.2%	2.5%	2.9%	4.6%

Root mean square error (RMS):

$$\mathrm{rms} = \sqrt{\frac{\sum_{i=1}^{n}\left(\mathrm{VB_{pi}} - \overline{VB_e}\right)^2}{n}}$$

Coefficient of variation (COV):

$$\mathrm{cov} = \frac{\mathrm{rms}}{|\overline{\mathrm{VB_e}}|}$$

$\overline{VB_e}$: Mean experimental flank wear

VB_{pi}: Predicted flank wear

Fig. 11 shows the scatter of data related to the values obtained from neural network models compared to the data obtained from experiments. The points shown on the diagrams indicate the percentage difference between the experimental values and the values obtained from the artificial neural network patterns for all data. This difference is calculated from the following formula:

$$\text{perediction error} = \frac{VB_e - VB_p}{VB_E} \times 100$$

Where VB_e is the experimental flank wear and VB_p is the flank wear were obtained from neural network patterns. Values greater than 0 are above the horizontal axis and values less than 0 are below the horizontal axis. As can be seen, except for a few points, for the rest of the points, the error range is 10%.

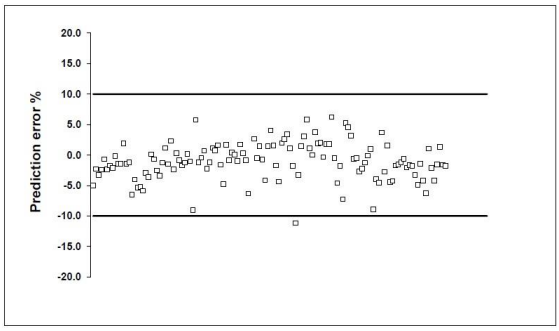

a) percentage error for experimental data & prediction based on ANN No.1

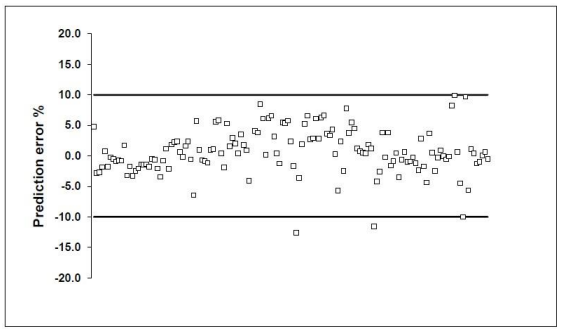

b) percentage error for experimental data & prediction based on ANN No.4

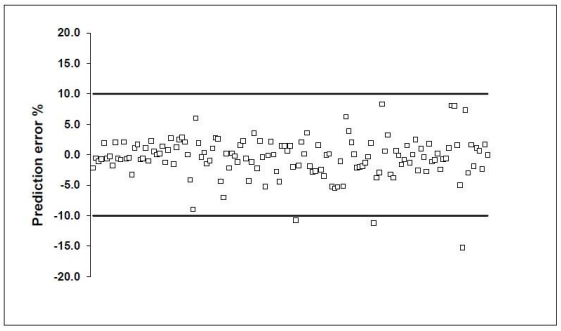

c) percentage error for experimental data & prediction based on ANN No.5

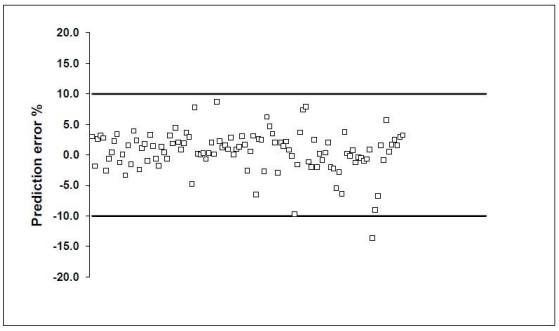

d) percentage error for experimental data & prediction based on ANN No.6

Fig. 11 percentage error for experimental data & prediction based on

4- Conclusion

From the total content of this research, the following results are obtained:

1- In the experimental range, there was a good correlation between the axial and radial cutting force components against flank wear. But the tangential component of the cutting force was less correlated with tool wear. For this reason, axial and radial components of cutting force were used in the construction of tool wear prediction patterns.

2- Cutting force components depend on the cutting conditions. They are also affected by tool wear and increase with increasing tool wear. To reduce the effect of cutting conditions on cutting force components, different cutting force component and cutting condition ratios were introduced. These ratios were used to obtain tool wear patterns in neural networks. The results of

the models showed the appropriate efficiency of these ratios.

3- The introduced force ratios were used in the development of neural network patterns. These patterns were developed through three-layer perceptron neural networks. The obtained patterns were able to predict tool wear with appropriate accuracy. Also, the results obtained from the models in which the axial component of the cutting force was used, were better than other models.

References

[1] Choudhury, S. K. and Kishore, K. K., (2000). Tool wear measurement in turning using force ratio. *International Journal of Machine Tools and Manufacture*, *40*, 899-909.

[2] Dan, L. and Mathew, J., (1990). Tool wear and failure monitoring techniques for turning-A review. International Journal of Machine Tools and Manufacture, 30, 579-598.

[3] Cook, N.H., (1980). Tool wear sensors. Wear, 62, 49-57.

[4] S. Dutta, S. K. Pal, S. Mukhopadhyay, R. Sen, (2013). Application of digital image processing in tool condition monitoring: a review. CIRP Journal of Manufacturing Science and Technology, 6(3), 212–232.

[5] Chalwa, R. and Datar, S. B., (1980). Deduction of flank and crater wear from measurements of the total volumetric wear rates of radioactive tools. *Wear*, *58*, 213-222.

[6] Choudhury, S. K., Jain, V. K. and Rama Rao, Ch. V. V, (1999). On-line monitoring of tool wear in turning using a neural network. *International Journal of Machine Tools and Manufacture*, *39*, 489-504.

[7] El Gomayal, J.I. and Bregger, K.D., (1986). On-line tool-wear sensing for turning operations. *Journal of Engineering for Industry*, *108(1)*, 44-47.

[8] Drouillet C, Karandikar J, Nath C, et al., (2016). Tool life predictions in milling using spindle power with the neural network technique. *Journal of Manufacturing Process*, *22*, 161–168.

[9] Cuppin, D., Derrico, G., and Rutelli, G., (2001). Tool wear monitoring based on cutting power measurement. *Wear*, *39(5)*, 981-992.

[10] N. Khanna, C. Agrawal, M. Dogra, C. I. Pruncu, (2020). Evaluation of tool wear, energy consumption, and surface roughness during turning of Inconel 718 using sustainable machining technique, *Journal of Materials Research and Technology*, *9(3)*, 5794-5804.

[11] Balla Srinivasa Prasad, M. Prakash Babu, (2017). Correlation between vibration amplitude and tool wear in turning: Numerical and experimental analysis, *Engineering Science and Technology, an International Journal*, *20(1)*, 197-211.

[12] P. Twardowski, M. Tabaszewski, M. W. Pikuła, A. F. Czyryca, (2021). Identification of tool wear using acoustic emission signal and machine learning methods, *Journal of the International Societies for Precision Engineering and Nanotechnology*, *72*, 738-744.

[13] Koren, Y. and Lenz, E., (1970). A mathematical model for the flank wear while turning steel with carbide tools, *CIRP seminar, Trondheim.*

[14] Sumit Kanti Sikdar, Mingyuan Chen, (2002). Relationship between tool flank wear area and component forces in single-point turning, *Journal of Materials Processing Technology*, *128(1)*, 210-215.

[15] V.S. Sharma, S.K. Sharma, A.K. Sharma, (2008). Cutting tool wear estimation for turning, *Journal of*

Intelligent Manufacturing, *19(1)*, 99–108.

[16] Jaharah A. Ghani, Muhammad Rizal, Mohd Zaki Nuawi, Che Hassan Che Haron, Mariyam Jameelah Ghazali, Mohd Nizam Ab Rahman, Online Cutting Tool Wear Monitoring using I-Kaz Method and New Regression Model, (2010*). Advanced Materials Research*, *126*, 738-743.

[17] Vallabh D. Patel, Anish H. Gandhi, (2019). Modeling of cutting forces considering progressive flank wear in finish turning of hardened AISI D2 steel with CBN tool, *The International Journal of Advanced Manufacturing Technology*, *104(1)*, 1-14.

[18] R. Baig, S. Javed, M. Khaisar, (2021). Development of an ANN model for prediction of tool wear in turning EN9 and EN24 steel alloy, *Advances in Mechanical Engineering*, *13(6)*, 1–14

[19] M. S. Alajmi, A. M. Almeshal, (2021). Modeling of Cutting Force in the Turning of AISI 4340 Using Gaussian Process Regression Algorithm, *Applied Sciences*, *11*, 4055.

[20] A. Siddhpura and R. Paurobally, (2013). A review of flank wear prediction methods for tool condition monitoring in a turning process, *The International Journal of Advanced Manufacturing Technology, 65(1–4)*, 371–393.

[21] G. Zhang, C. Guo, (2016). Modeling Flank Wear Progression Based on Cutting Force and Energy Prediction in Turning Process, *Procedia Manufacturing*, *5*, 536–545.

[22] M. Hanief, M.F. Wani, M.S. Charoo, (2017). Modeling and prediction of cutting forces during the turning of red brass (C23000) using ANN and regression analysis, *Engineering Science and Technology*, *20*, 1220–1226.

[23] Kolahdooz, A. & Loh-Mousavi, M. (2015). Optimization of Microstructure and Mechanical Properties of Al-A360 Produced by Semi-Solid Casting, *Journal of Simulation and Analysis of Novel Technologies in Mechanical Engineering*, *8(1)*, 59-71, (in Persian).

[24] Manoochehri M. & Kolahan, F. (2014). Integration of artificial neural network and simulated annealing algorithm to optimize deep drawing process, *International Journal of Advanced Manufacturing Technology*, *73(1)*, 241-249.

[25] Zohoor, M., Shahverdi, H. Tafakori, A., (2010). Optimization of Flash, Billet Dimensions and Friction Factor in Closed Die Cold Forging Process, *Journal of Simulation and Analysis of Novel Technologies in Mechanical Engineering*, *3(1)*, 71-80, (in Persian).

[26] M. Azimi, A. Kolahdooz, S.A. Eftekhari, (2016). Optimization of Material Removal Rate in Electrical Discharge Machining Alloy on DIN1.2080 with the Neural Network and Genetic Algorithm, *Journal of Simulation and Analysis of Novel Technologies in Mechanical Engineering*, *9(1)*, 77-92, (in Persian).

[27] Menhaj M.B. (2000). fundamentals of neural networks vol. 1: Computational intelligence. Amirkabir University of Technology Press, (in Persian).

[28] Woong Youn, J. and Yang Yang, M., (2001). A study on the relationships between static/dynamic cutting force components and tool wear, *Journal of Manufacturing Science and Engineering*, *123*, 196-205.